International Journal of Agricultural and Environmental Information Systems
Volume 13 • Issue 1

Spatiotemporal Evolution of NPP in Sandy Land of China's Seasonal Freezing-Thawing Typical Region

Jingfa Wang, Jilin Normal University, China
Huishi Du, Jilin Normal University, China*

ABSTRACT

Based on the data set of AVHRR GIMMS, TERRA/AQUA MODIS NDVI, and climate data from 1982 to 2018, CASA model, GIS spatial analysis, and mathematical statistics were used to study the changing law in the category of time and space, spatial distribution, and the correlativity between the NPP and meteorological factors in the sandy land of China's Seasonal Freezing-Thawing Typical Region. The results showed that the average annual NPP value of vegetation in the growing season of the sandy land from 1982 to 2018 fluctuated between 217.65-356.61 gC/m^2a, showing an obvious seasonality and a significant increase. The spatial distribution of NPP in the sandy land in the near 37a is significantly different. There are significant seasonal differences in vegetation responses to temperature, precipitation, wind speed, evaporation, and other meteorological factors in different regions. The increase of vegetation cover in sandy land of China's Seasonal Freezing-Thawing Typical Region is controlled by regional atmospheric circulation and human dynamics.

KEYWORDS

Driving Force, NPP, Seasonal Freezing-Thawing Typical Region, Space-Time Evolution

INTRODUCTION

In the global ecosystem, vegetation has important indication function in the conservation of soil erosion, regulation of the atmosphere, maintenance of climate, and stability of the entire ecosystem (Richards et al., 2022; Song et al., 2021). Net primary productivity (NPP) can directly represent the apparent changes of ecological environment and ecosystem production capacity, and can be reflected in the process of environmental climate change in geophysics and biogeochemistry (Becknell et al., 2021; Zhou et al., 2022). NPP is important index functions to study various terrestrial ecological processes (Chen et al., 2021). Accurate monitoring of regional NPP has important practical application value for the assessment of vegetation resource changes, exploration of vegetation production potential, and rational utilization of resources (Zhang et al., 2020). It is the important core content of research on contemporary earth material circulation science to estimate regional ecosystem vegetation NPP, quantitatively study its spatiotemporal change characteristics, and analyze its relationship with climate

DOI: 10.4018/IJAEIS.312254 *Corresponding Author

change (Jin et al., 2020). Therefore, the measurement and evaluation of NPP on a global scale or in a specific region has attracted much attention from researchers (Wei et al., 2022). Remote sensing model estimation is an effective method to obtain NPP on a large scale, quickly and accurately (Ge et al., 2022). During the years 1965-1974, scholars from various countries established the CASA, Miami, Thornthwaite, Chikugo, and other models by combining measured data with climate and environmental factors, and conducted a large number of assessments and tests on NPP (Liu et al., 2022). Among the many regional terrestrial NPP estimation models, the CASA model is simple and practical, and is one of the most potential research methods (Zhang et al., 2021).

Freezing-thawing erosion area refers to an area characterized by strong freezing-thawing action and corresponding landform of freezing-thawing erosion (Tao et al., 2021). The sands in China's seasonal freezing-thawing typical region are located at the northeast sea-land transition zone of the Eurasian continental mid-latitude giant sand belt and the eastern edge of China's sandy desertification land, and the regional climate and human activities have regional characteristics (Gao et al., 2021). Researchers in China have conducted much work on freeze-thaw area vegetation NPP (Wang et al., 2021). However, most of the research scholars have studied specific study areas, short time series NPP, and its influencing factors, and relatively few studies have been conducted on the spatial distribution of long time series NPP and significant and potential factors affecting NPP changes in the sandy areas of the freezing-thawing erosion area of China. Therefore, in this paper, the authors chose the sand in China's seasonal freezing-thawing typical region as their research object. They used AVHRR GIMMS, TERRA/AQUA MODIS NDVI data, and the more time and space scales to calculate the sand vegetation NPP dynamic change trend between whole and parts, combined them with meteorological data such as temperature, precipitation, wind speed, and evaporation, and discussed the sand vegetation NPP dynamic evolution and drive. To clarify the change process and driving force of NPP in spatiotemporal evolution of NPP in sandy land of China's seasonal freezing-thawing typical region, the paper provides basic data for the further implementation of ecological restoration project and ecological civilization construction.

BACKGROUND OF THE RESEARCH AREA

The total sand area of the spatiotemporal evolution of NPP in sandy land of China's seasonal freezing-thawing typical region the authors studied in this paper is about 423,763.35 km^2, located at 42°30' - 50°40'N and 115°30' - 129°10'E, including Horqin, Songnen, and Hulun Buir sandy land (Figure 1). Horqin sandy land of 64 387.22 km^2 is located in 42°30' - 44°50'N, 118°30' - 124°15'E. The average temperature per year is 5.2 - 6.4°C and the annual precipitation is 343 - 500 mm. Songnen sandy land was at 43°00' - 50°40'N, 119°20' - 129°10'E and with an area of 352,559.12 km^2. The average temperature per year is 3.3°C and the average precipitation per year is 360-480 mm. Landscape was mainly fixed sand dune. Plants included *Ulmus pumila L.*, *Armeniaca sibirica (L.) Lam.*, *Stipa grandis P. Smirn.*, *Artemisia halodendron Turcz. exBess.*, and *Caragana microphylla Lam.* Hulun Buir sandy land was at 46°40' - 50°20'N, 115°30' - 122°25'E and with an area of 6,817.01 km^2. The average temperature per year is 2.5°C and the annual precipitation is 280 - 400 mm.

DATA AND METHODS

Data Source and Processing

GIMMS NDVI data using NASA global testing with the model group (GIMMS) provide GIMMS NDVI and biggest synthetic data, time series of 1982-2006, the data set is currently the longest time series of NDVI data (Ali et al., 2020). MODIS NDVI data adopt MOD13A2 data products from NASA'S EOS/MODIS NDVI data (https://lpdaac.usgs.gov), and the time series is 2001-2021 (Yan et al., 2022). Since GIMMS and MODIS have different sensors, significant differences exist in near-

Figure 1. The location and boundary of study area

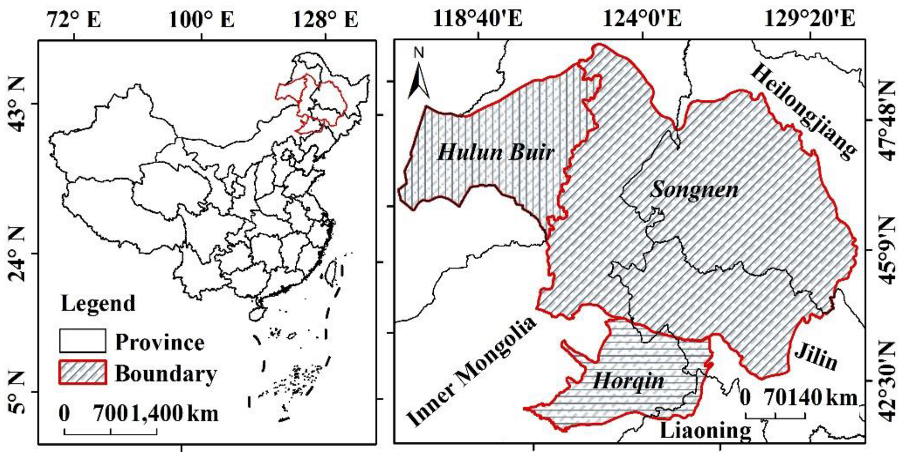

infrared band, red band, and temporal and spatial resolution, so it is necessary to check and verify the consistency of the two NDVI data before data interpolation and fusion. The correlation analysis of the overlapping annual growing season vegetation NDVI data of AVHRR GIMMS, TERRA/AQUA MODIS NDVI from 2001 to 2006, showed that the correlation coefficient was 0.894.

Meteorological collection data are from China Meteorological Data Processing Center (http://www.gscloud.cn), including monthly average temperature, total precipitation, and total solar radiation data of 110 stations in Heilongjiang, Jilin, and Inner Mongolia, from 1982 to 2021.

METHODS

Maximum Value Composites

In order to analyze the regional vegetation and NDVI variation characteristics of overall in time and space, the maximum value composites to obtain maximum NDVI, vegetation index reflects a certain period of time in the best state, which can effectively reduce from aerosol, cloud shadow, and perspective, such as noise, reduce the error, and improve the accuracy of vegetation index and quality.

Mean Value Method

In order to reflect the average level of NDVI in the study area, in this paper the authors adopted the mean value method to statistically analyze the mean value of NDVI in China's seasonal freezing-thawing typical region (Cai et al., 2022). The mean value method is an indicator reflecting the central trend of data. It can effectively calculate the average NDVI of vegetation in each specific time period in the study area.

Carnegie-Ames-Stanford Approach Model

The NPP estimated in the CASA model can be represented by the factors of available photosynthetic radiation absorbed, stored, and utilized by plants and the efficiency of solar energy absorption, conversion, and utilization (ε). Using remote sensing images to estimate that the part of the plant's absorption of photosynthetic effective radiation is achieved based on the reflection characteristics of the infrared and near-infrared wavelengths of vegetation. Photosynthetic effective radiation is the driving force of photosynthesis, which has a strong correlation with biomass (Zhang et al., 2021).

Grey Relational Analysis

The correlation degree is a measure of the correlation between two systems or two factors. Only a small amount of time series data is needed to analyze the relationship between the elements in the system, which avoids the shortage of correlation analysis based on the random process of probability theory that requires a large number of data samples (Cao et al., 2022).

Correlation Analysis

The geographical elements are always interdependent, interrelated, and mutually restricted. Correlation analysis is a universal method to study the relationship among these geographical elements, which includes two parts: Correlation direction and correlation degree (Mo & Ren, 2020).

RESULTS AND ANALYSIS

Spatiotemporal Evolution of Net Primary Productivity

Variation Characteristics of Sand Net Primary Productivity Time Series

The NPP of sandy land vegetation growing season in China's seasonal freezing-thawing typical region from 1982 to 2021 is between 217.65 and 356.61 gC/m^{2}a, and the average is 303.19 gC/m^{2}a, slightly lower than the national average of NPP of the same period (Figure 2A). The NPP of sandy land showed an overall trend of fluctuating increase, with a determination coefficient

Figure 2. Interannual trend of NPP in China's seasonal freezing-thawing typical region (A: Sand mass in China's Seasonal Freezing-Thawing Typical Region; B: Horqin; C: Songnen; D: Hulun Buir)

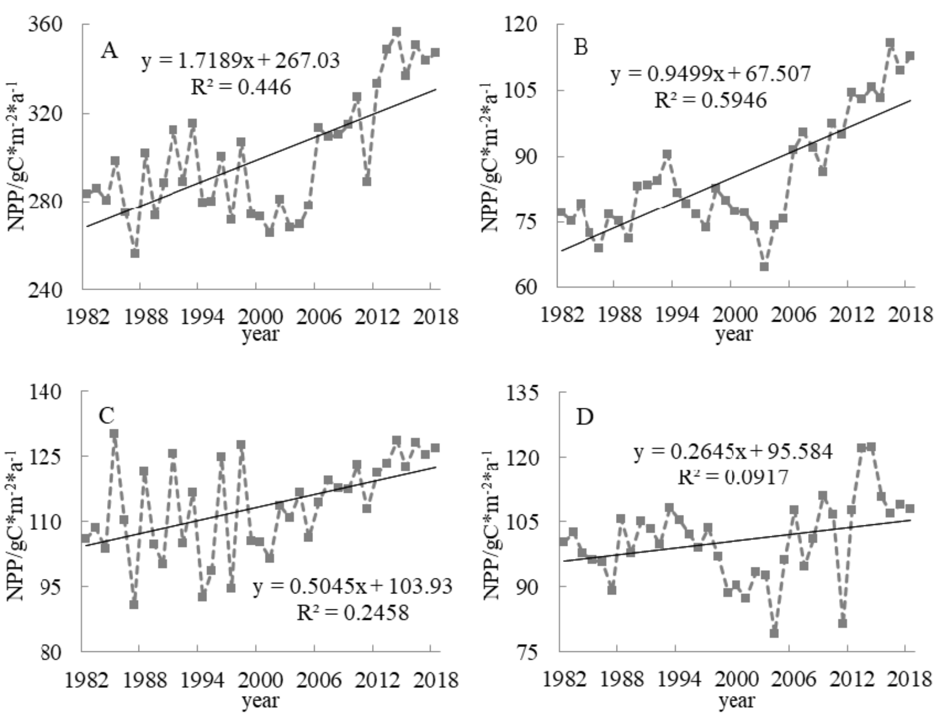

R^2 of 0.5349 and a linear fitting increase slope of 1.8475. The linear increase was significant, with an average annual increase of 1.63 gC/m^{2}a. In 2014, the average NPP per year of sandy land vegetation was the largest, 356.61 gC/m^{2}a. In 2014, there was sufficient precipitation, abundant solar radiation, and superior vegetation growth conditions in the study area, leading to an obvious increase in the carbon accumulation content of vegetation. In 1986, the annual mean NPP of the overall vegetation in China's seasonal freezing-thawing typical region was the smallest, only 217.65 gC/m^{2}a. The monthly mean temperature in the spring of 1986 in Songnen Sandy land was lower, 1.5°C lower than the monthly mean temperature in the spring of 1985, leading to poor vegetation growth in that year. In 1986 and 1987, NPP value was lower than 260 gC/m^{2}a. In 2014 and 2016, NPP value was higher than 350 gC/m^{2}a. From 1982 to 2021, the NPP of the vegetation in Horqin sandy land ranged from 64.66 to 115.87 gC/m^{2}a, and the average was 87.52 gC/m^{2}a. The overall growth was significant, with an average annual growth of 0.89 gC/m^{2}a, with an increase of 44.76% (Figure 2B). From 1982 to 2021, the NPP of Songnen Sandy land was between 53.26 and 130.07 gC/m^{2}a, and the average was 114.47 gC/m^{2}a. The overall fluctuation was significant, with an average annual growth of 0.52 gC/m^{2}a, with an increase of 19.01% (Figure 2C). From 1982 to 2021, the NPP of the vegetation in Hulun Buir Desert ranged from 79.02 to 171.37 gC/m^{2}a, and the average was 101.20 gC/m^{2}a (Figure 2D). The overall fluctuation increased significantly, with an average annual growth of 0.23 gC/m^{2}a, with an increase of 8.89%.

The vegetation NPP growing season in the freezing-thawing erosion area of China for nearly 40a showed different levels of growth trends at different growth rates in each season. Overall, the average NPP in the study area was 152.92 gC/m^{2}a, 508.23 gC/m^{2}a, and 151.37 gC/m^{2}a in spring, summer, and autumn, respectively, and it was clear that the NPP of vegetation in the freezing-thawing erosion area of China was the largest in the summer growing season, followed by autumn, and finally spring (Figure 3A). The mean NPP of vegetation in Horqin sandy land in spring is 36.79 gC/m^{2}a, which increases from 22.81 gC/m^{2}a in 1982 to 64.51 gC/m^{2}a in 2021(Figure 3B). The average NPP of spring vegetation in Songnen sandy land is 64.31 gC/m^{2}a, which increases from 52.59 gC/m^{2}a in 1982 to 96.22 gC/m^{2}a in 2021 (Figure 3C). The average NPP of the vegetation in Hulun Buir desert in spring is 51.66 gC/m^{2}a, which increases from 36.73 gC/m^{2}a in 1982 to 63.25 gC/m^{2}a in 2021 (Figure 3D).

Spatial Evolution Characteristics of Net Primary Productivity in Sandy Land

The annual mean value of NPP in most areas near 40a is above 43.75 gC/m^{2}a, and the vegetation is in good condition, while the annual mean value of NPP in most areas in the southwest is between 14.33 and 28.17 gC/m^{2}a, and the vegetation is in poor condition (Figure 4A). In the 2021 vegetation growing season of Songnen Sandy land, NPP ranges from 0.02 to 127.29 gC/m^{2}a. In the recent 40 years, the annual mean value of NPP in most areas has been above 44.75 gC/m^{2}a, with good vegetation condition, while the annual mean value of NPP in central and southern areas has been mostly between 13.17 and 35.65 gC/m^{2}a, with relatively poor vegetation condition. The NPP of the vegetation in Hulun Buir Desert ranges from 0.08 to 101.11 gC/m^{2}a, and gradually increases from the west to the east. Horqin growing season vegetation NPP is obviously a rising trend, the increase is 15.85-31.65 gC/m^{2}a, but the space difference is bigger; among them, most parts of NPP increase is small, change value is between 10.65 and 21.35 gC/m^{2}a, only Naiman, Kailu, central and southern Keerqinzuoyizhongqi and Keerqinzuoyihouqi, and other regions, the addition of NPP is 31.65-50.05 gC/m^{2}a, the degree of change is relatively large (Figure 4B). In the growing season, the NPP decreased mainly in the eastern part of Kulun, the southern part of Keerqinyouyizhongqi, and the northern part of Alukeerqin. The decrease was between 8.65 and 17.55 gC/m^{2}a.

Figure 3. Seasonal variation characteristics of NPP in China's seasonal freezing-thawing typical region (A: Sand mass in China's seasonal freezing-thawing typical region; B: Horqin; C: Songnen; D: Hulun Buir)

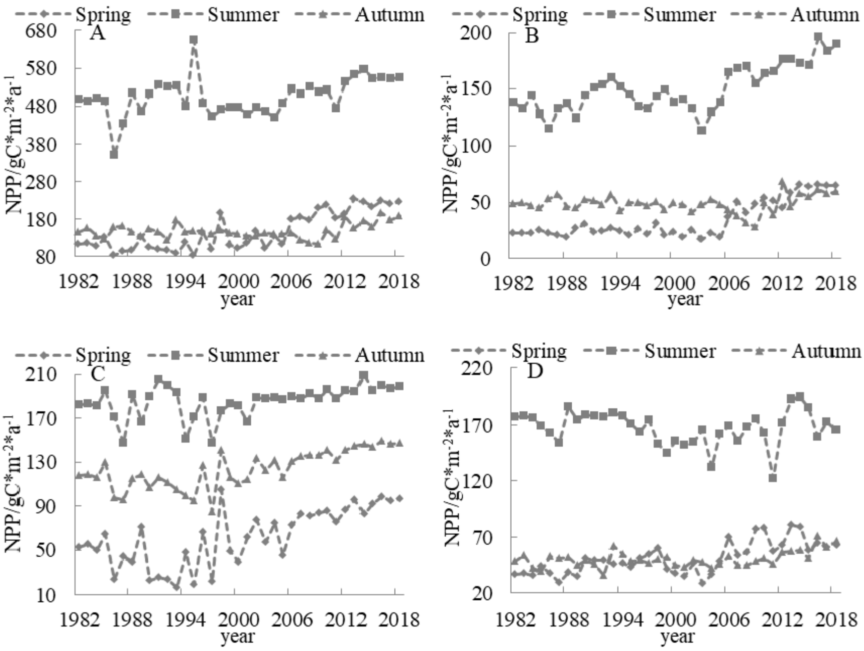

Figure 4. Perennial mean (A) and variable (B) spatial distribution of NPP in China's seasonal freezing-thawing typical region

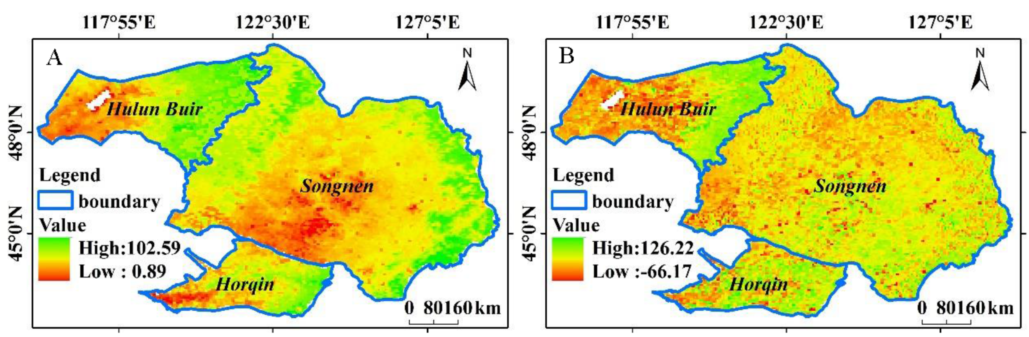

ANALYSIS OF CLIMATE DRIVING FORCE OF SPATIOTEMPORAL EVOLUTION OF SANDY NET PRIMARY PRODUCTIVITY

Climate Change Characteristics

The mutual influence and interaction between climate and vegetation bring up the geographical phenomenon on a small regional scale, and even on a large earth energy transformation and flow scale. The annual mean air temperature in this sandy land of China's seasonal freezing-thawing typical region showed a general fluctuation trend (Figure 5A). The change of annual average precipitation is mainly divided into two stages: The average precipitation fluctuated steadily

Figure 5. Meteorological elements of sand in China's seasonal freezing-thawing typical region (A: Annual mean temperature; B: Average annual precipitation; C: Annual average wind speed; D: Annual evaporation)

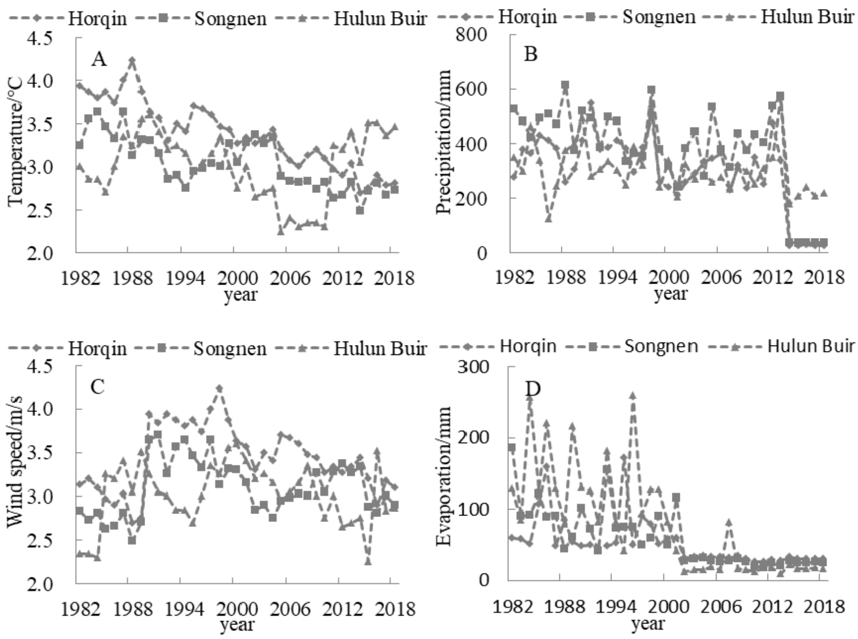

from 1982 to 2013, decreased significantly from 2014 to 2018, and began to rebound after 2018 (Figure 5B). The change of annual average wind speed can be divided into two stages: From 1982 to 1998, the average wind speed fluctuates upward, and, from 1998 to 2021, it fluctuates downward (Figure 5C). The change of annual average evaporation showed a downward trend, with a large change range from 1982 to 2000, and the evaporation decreased significantly after 2000 (Figure 5D).

Relationship Between Net Primary Productivity and Climatic Factors

The grey correlation was all greater than 0.3, indicating that there was a great correlation between vegetation index changes and natural factors (Table 1). The grey correlation between Horqin and Songnen sandy land and meteorological factors is the average wind speed per year and has the strongest influence, followed by the average temperature per year and average precipitation per year; the average evaporation per year has the least influence. Hulun Buir sandy land is the most correlated

Table 1. NPP grey relational analysis in China's seasonal freezing-thawing typical region

Factors	Horqin		Songnen		Hulun Buir	
	Grey Relational Degree	Correlation Order	Grey Relational Degree	Correlation Order	Grey Relational Degree	Correlation Order
Wind speed	0.6468	1	0.6908	1	0.6375	2
Temperature	0.5671	2	0.6397	2	0.7226	1
Precipitation	0.4879	3	0.5146	3	0.5726	3
Evaporation	0.4504	4	0.3352	4	0.3254	4

with average temperature per year, followed by average wind speed per year, average precipitation per year, and average evaporation per year.

The absolute value of correlation coefficient between vegetation NPP and climatic factors in Horqin sandy land is the maximum average per year temperature, followed by average precipitation per year, and, finally, average evaporation per year and average wind speed per year (Table 2). The absolute value of the correlation coefficient between vegetation NPP and climatic factors in Songnen Sandy land is also the largest average temperature per year, followed by average evaporation per year, and, finally, average precipitation per year and average wind speed per year. The absolute value of the correlation coefficient between vegetation NPP and weather change factors in Hulun Buir sandy land is the maximum average precipitation per year, followed by average temperature per year, average evaporation per year, and average wind speed per year.

DISCUSSION

Net Primary Productivity Time Change

From 1982 to 2021, NPP in the sandy land vegetation growing season in China's seasonal freezing-thawing typical region presented an overall trend of fluctuation and increase, which is similar to the results on the variation trend of NPP at different scales in the world, the global arid region, Eurasia, China, and eastern China (Gang et al., 2016; Shi & Wang, 2015; Yang et al., 2016; Zhong et al., 2016). Compared with the period 1986-2005, the change process of NPP in the growing season of sandy land vegetation in China's seasonal freezing-thawing typical region in the 21st century was also basically similar to the results of Shi and Wang (2015) and Gang et al. (2016) in the NPP in the global grassland and midhigh latitudinal regions of the Northern Hemisphere, at the same time as the change of NPP in the Chinese mainland. However, due to the extension of the study period, the trend of increase in the latter period was more obvious. From 1992 to 2005, there was no significant decrease trend of NPP in the growing season of sandy land vegetation in China's seasonal freezing-thawing typical region, which was basically similar to the results of Gao (2013) studying on spatial-temporal variation of vegetation carbon flux from 1901 to 2005 and using the NPP values of vegetation from the seven Earth system models. From 2005 to 2021, NPP increased significantly in the sandy land vegetation growth season in China's seasonal freezing-thawing typical region, which was basically consistent with the research results of Zhou et al. (2017) and Zhang et al. (2014) in China and eastern China. The opposite trend of NPP in the growth season of sandy land vegetation in China's seasonal freezing-thawing typical region around 1992 and the significant increase after 2005 was mainly caused by the corresponding change of NPP in summer.

Net Primary Productivity Spatial Evolution

The spatial distribution of NPP in China's seasonal freezing-thawing typical region from 1982 to 2021 is consistent with the results of Mu et al. (2013), Wang et al. (2020), and Parihar et al. (2020) in China and Inner Mongolia. However, according to Mu et al. (2013), the spatial distribution of

Table 2. Correlation coefficient between the NPP and climatic factors in China's seasonal freezing-thawing typical region

Sand	Temperature		Precipitation		Wind Speed		Evaporation	
	C	S	C	S	C	S	C	S
Horqin	-0.788	0.017	-0.553	0.016	-0.113	0.506	-0.488	0.012
Songnen	-0.421	0.011	-0.262	0.117	-0.201	0.233	-0.355	0.031
HulunBuir	0.208	0.217	-0.458	0.521	0.109	0.014	-0.188	0.266

Note: C = correlation; S = Significant

NPP in Inner Mongolia is mainly manifested in the change of longitude zone, and the change rate from west to east is increased by 200.5 $gC/m^2a/10°$. Jiang et al. (2020) believed that the whole is getting better and greener and the part is getting worse and degraded of NPP in the farming-pastoral ecotone in the period 2000-2015 resulted in a significant degradation rate of 0.39%. In this paper, the authors chose Horqin, Songnen, and Hulun Buir as their research objects, which belong to a physical geographical unit, thus promoting the in-depth study of the northeast and the west. This study shows that the annual change of NPP value in different regions presents a single-peak curve, which starts to increase in May, reaches its peak in July, and begins to decline in a wide range in September. On the spatial scale, NPP value showed a large area of fluctuation and increase trend, which was also basically consistent with the results of image-by-pixel analysis by Conradi et al. (2020) and Guo et al. (2021).

CONCLUSION

From 1982 to 2021, the average annual NPP value in the sandy land growing season of China's seasonal freezing-thawing typical region fluctuated between 217.65 and 356.61 gC/m^2a. After 2000, the region gradually developed towards ossification.

The spatial distribution of NPP of sandy land vegetation is obviously different. In the nearest 40 years, the NPP in Horqin sandy land ranged from 64.66 to 115.87 gC/m^2a, and the perennial average was 85.56 gC/m^2a. The NPP of vegetation in Songnen sandy land ranged from 53.26 to 130.07 gC/m^2a, and the perennial average was 111.98 gC/m^2a. The NPP of vegetation in Hulun Buir sandy land ranged from 79.02 to 171.37 gC/m^2a.

There is a significant correlation between temperature and precipitation and NPP in the study area. From a statistical perspective, socioeconomic factors play a major function in the evolution law of NPP in sandy land, which is significantly affected by urbanization.

FUNDING

This research was funded by the National Natural Science Foundation of China (NO. 41871022).

CONFLICT OF INTEREST

The authors declare that they have no conflicts of interest to report regarding the present study.

REFERENCES

Ali, S., Henchiri, M., Sha, Z., Wilson, K., Yun, B., Yao, F. M., & Zhang, J. H. (2020). A time series of land cover maps of South Asia from 2001 to 2015 generated using AVHRR GIMMS NDVI3g data. *Environmental Science and Pollution Research International*, *27*(16), 20309–20320. doi:10.1007/s11356-020-08433-9 PMID:32239413

Becknell, J. M., Vargas, G. G., Pérez-Aviles, D., Medvigy, D., & Powers, J. S. (2021). Above-ground net primary productivity in regenerating seasonally dry tropical forest: Contributions of rainfall, forest age and soil. *Journal of Ecology*, *109*(11), 3903–3915. doi:10.1111/1365-2745.13767

Cai, T. T., Yu, D. M., Liu, H. N., & Gao, F. K. (2022). Computational analysis of variational inequalities using mean extra-gradient approach. *Mathematics*, *10*(13), 2318. doi:10.3390/math10132318

Cao, W., Xuan, X. D., Wu, W. D., Chen, L. H., & Zhang, Q. Y. (2022). A new method for determining the optimal adaptive thermal comfort model with grey relational analysis. *Building and Environment*, *221*, 109277. doi:10.1016/j.buildenv.2022.109277

Chen, S. T., Guo, B., Zhang, R., Zang, W. Q., Wei, C. X., Wu, H. W., Yang, X., Zhen, X. Y., Li, X., Zhang, D. F., Han, B. M., & Zhang, H. L. (2021). Quantitatively determine the dominant driving factors of the spatial: Temporal changes of vegetation NPP in the Hengduan Mountain area during 2000-2015. *Journal of Mountain Science*, *18*(2), 427–445. doi:10.1007/s11629-020-6404-9

Conradi, T., Van, M. K., Ordonez, A., & Svenning, J. (2020). Biogeographic historical legacies in the net primary productivity of Northern Hemisphere forests. *Ecology Letters*, *23*(5), 800–810. doi:10.1111/ele.13481 PMID:32086879

Gang, C. C., Wang, Z. Q., Yang, Y., Chen, Y. Z., Zhang, Y. Z., Li, J. L., & Cheng, J. M. (2016). The NPP spatiotemporal variation of global grassland ecosystems in response to climate change over the past 100 years. *Caoye Xuebao*, *25*(11), 1–14. doi:10.11686/cyxb2016148

Gao, X. F., Shi, X. N., & Lei, T. W. (2021). Influence of thawed soil depth on rainfall erosion of frozen bare meadow soil in the Qinghai-Tibet Plateau. *Earth Surface Processes and Landforms*, *46*(10), 1953–1963. doi:10.1002/esp.5138

Gao, Y. S. (2013). Discussion on the effect of hulunbuir sandy land management on ecological environment. *Inner Mongolia Forestry Investigation and Design*, *36*(2), 41–42. doi:10.13387/j.cnki.nmld.2013.02.057

Ge, W. Y., Deng, L. Q., Wang, F., & Han, J. Q. (2021). Quantifying the contributions of human activities and climate change to vegetation net primary productivity dynamics in China from 2001 to 2016. *The Science of the Total Environment*, *773*, 145648. doi:10.1016/j.scitotenv.2021.145648 PMID:33582337

Guo, X. M., Tong, S. Q., Ren, J. Y., Ying, H., & Bao, Y. H. (2021). Dynamics of vegetation net primary productivity and its response to drought in the Mongolian Plateau. *Atmosphere*, *12*(12), 1587–1599. doi:10.3390/atmos12121587

Jiang, H. L., Xu, X., Guan, M. X., Wang, L. F., Huang, Y. M., & Jiang, Y. (2020). Determining the contributions of climate change and human activities to vegetation dynamics in agro-pastural transitional zone of northern China from 2000 to 2015. *The Science of the Total Environment*, *718*, 134871. doi:10.1016/j.scitotenv.2019.134871 PMID:31839307

Jin, H., Bao, G., Chen, J. Q., Chopping, M., Jin, E., Mandakh, U., Jiang, K., Huang, X. J., Bao, Y. H., & Vandansambuu, B. (2020). Modifying the maximal light-use efficiency for enhancing predictions of vegetation net primary productivity on the Mongolian Plateau. *International Journal of Remote Sensing*, *41*(10), 3740–3760. doi:10.1080/01431161.2019.1707902

Liu, W. R., Li, X. T., Li, T., & Jia, B. Q. (2022). Spatiotemporal variations of forest NPP and related driving factors based on MODIS and CASA models in Yichun. *Shengtaixue Zazhi*, *41*(1), 150–158. doi:10.13292/j.1000-4890.202201.026

Mo, J. H., & Ren, F. (2020). Discrete element analysis on the correlation between marketing means and economic benefits of island ecotourism. *Journal of Coastal Research*, *103*(sp1), 1038–1041. doi:10.2112/SI103-216.1

Mu, S. J., Li, J. L., Zhou, W., Yang, H. F., Zhang, C. B., & Ju, W. M. (2013). Spatial-temporal distribution of net primary productivity and its relationship with climate factors in Inner Mongolia from 2001 to 2010. *Acta Ecologica Sinica*, *33*(12), 3752–3764. doi:10.5846/stxb201205030638

Parihar, M., Rakshit, A., Meena, V. S., Gupta, V. K., Rana, K., Choudhary, M., Tiwari, G., Mishra, P. K., Pattanayak, A., Bisht, J. K., Jatav, S. S., Khati, P., & Jatav, H. S. (2020). The potential of arbuscular mycorrhizal fungi in C cycling: A review. *Archives of Microbiology*, *202*(7), 1581–1596. doi:10.1007/s00203-020-01915-x PMID:32448964

Richards, D. R., Belcher, R. N., Carrasco, L. R., Edwards, P. J., Fatichi, S., Hamel, P., Masoudi, M., McDonnell, M. J., Peleg, N., & Stanley, M. C. (2022). Global variation in contributions to human well-being from urban vegetation ecosystem services. *One Earth*, *5*(5), 522–533. doi:10.1016/j.oneear.2022.04.006

Shi, H. X., & Wang, C. H. (2015). Change of NPP at the mid-high latitude of Northern Hemisphere in the 21st century and its relation with climate factors. *Bingchuan Dongtu*, *37*(2), 327–335. doi:10.7522/j.issn.1000-0240.2015.0036

Song, G., Wang, B. Y., Sun, J. Y., Wang, Y. L., & Li, X. R. (2021). Response of revegetation to climate change with meso-and micro-scale remote sensing in an arid desert of China. *Sciences in Cold and Arid Regions*, *13*(1), 43–52. doi:10.3724/SP.J.1226.2021.20030

Tao, J., Ghantous, R. M., Jin, M., & Weiss, J. (2021). Influence of silica fume on freezing-and-thawing resistance of cement paste at early age. *ACI Materials Journal*, *118*(2), 107–116. doi:10.14359/51730414

Wang, T., Yang, M. H., Yan, S. J., Geng, G. P., Li, Q. H., & Wang, F. (2021). Effects of temperature and precipitation on spatiotemporal variations of net primary productivity in the Qinling Mountains, China. *Polish Journal of Environmental Studies*, *30*(1), 409–422. doi:10.15244/pjoes/122839

Wang, Y., Yue, H., Peng, Q., He, C., Hong, S., & Bryan, B. A. (2020). Recent responses of grassland net primary productivity to climatic and anthropogenic factors in Kyrgyzstan. *Land Degradation & Development*, *31*(16), 2490–2506. doi:10.1002/ldr.3623

Wei, X. D., Yang, J., Luo, P. P., Lin, L. G., Lin, K. L., & Guan, J. M. (2022). Assessment of the variation and influencing factors of vegetation NPP and carbon sink capacity under different natural conditions. *Ecological Indicators*, *138*, 108834. doi:10.1016/j.ecolind.2022.108834

Yan, J. N., He, H. X., Wang, L. Z., Zhang, H., Liang, D., & Zhang, J. Q. (2022). Inter-comparison of four models for detecting forest fire disturbance from MOD13A2 time series. *Remote Sensing*, *14*(6), 1446. doi:10.3390/rs14061446

Yang, Y. Z., Ma, Y. D., Jiang, H., Zhu, Q. A., Liu, J. X., & Peng, C. H. (2016). Evaluating the carbon budget pattern of Chinese terrestrial ecosystem from 1960 to 2006 using Integrated Biosphere Simulator. *Acta Ecologica Sinica*, *36*(13), 3911–3922. doi:10.5846/stxb201410262092

Zhang, M. L., Jiang, W. L., Chen, Q. G., & Liu, X. N. (2014). Estimation of grassland net primary production in China with improved CASA model based on the CSCS. *Journal of Desert Research*, *34*(4), 1150–1160. doi:10.7522/j.issn.1000-694X.2013.00414

Zhang, S., Bai, Y., Liu, Q., Tong, D. M., Xu, Z. T., Zhao, N., Wang, Z. X., Wang, X. P., Li, Y. S., & Zhang, J. H. (2021). Estimations of winter wheat yields in Shandong Province based on remote sensed vegetation indices data and CASA model. *Guangpuxue Yu Guangpu Fenxi*, *41*(1), 257–264. doi:10.3964/J.ISSN.1000-0593(2021)01-0257-08

Zhang, W., Ma, J., Liu, M., & Li, C. L. (2020). Impact of urban expansion on forest carbon sequestration: A study in Northeastern China. *Polish Journal of Environmental Studies*, *29*(1), 451–461. doi:10.15244/pjoes/102366

Zhong, X. C., Chen, W., Liu, T., Hao, X. N., Li, Z. M., & Sun, C. M. (2016). Spatial and temporal variation of NPP in China from 2001 to 2010 and its relationship with climate. *Zhongguo Nongye Ziyuan Yu Quhua*, *37*(9), 16–22. doi:10.7621/cjarrp.1005-9121.20160904

Zhou, W., Mou, F. Y., Gang, C. C., Guan, D. J., He, J. F., & Li, J. L. (2017). Spatial and temporal dynamics of net primary productivity of grassland in China from 1982 to 2010 and its relationship with climatic factors. *Acta Ecologica Sinica*, *37*(13), 4335–4345. doi:10.5846/stxb201408291724

Zhou, Z., Liang, M. J., Chen, L., Xu, M. P., Chen, X., Geng, L., Li, H., Serrano, D., Zhang, H. Y., Gong, Z., & Zhang, C. K. (2022). Processes, feedbacks, and morphodynamic evolution of tidal flat–marsh systems: Progress and challenges. *Water Science and Engineering*, *15*(2), 89–102. doi:10.1016/j.wse.2021.07.002

Jingfa Wang is a master student at Jilin Normal University.

Huishi Du is a professor at Jilin Normal University and the corresponding author.